Two-photon absorption spectra of GaAs with $2\hbar\omega_1$ near the direct band gap

J. P. van der Ziel
Bell Laboratories, Murray Hill, New Jersey 07974
(Received 8 April 1977)

The two-photon absorption spectrum of GaAs was measured at 300 and 4°K by monitoring the resulting band gap luminescence. For $2\hbar\omega_1$ more than 0.01 eV above the direct band gap E_g the luminescence has an approximately $(2\hbar\omega_1 - E_g)^{3/2}$ dependence characteristic of the allowed-forbidden mechanism corresponding to the two-band model. A weaker spectral dependence is observed when $2\hbar\omega - E_g < 0.01$ eV. This is tentatively identified with a contribution from the allowed-allowed mechanism of the three-band model which has an $\sim(2\hbar\omega - E_g)^{1/2}$ dependence, and exciton contributions in the continuum. The transition to the $n = 1$ exciton is weak, and is attributed to the allowed-allowed transition of the three-band model.

I. INTRODUCTION

We have measured the two-photon absorption (TPA) spectrum of GaAs by monitoring the band-gap luminescence as the energy of the pump is varied in the region of half the band-gap energy. There have been several previous measurements of the TPA absorption in GaAs using Nd laser radiation,[1-7] which is well above half the band-gap energy, and coefficients from[3] 0.02 cm/MW to[5] 5.6 cm/MW have been obtained. The most careful measurements have been made by Kleinman *et al.*[7] who obtained a value of 0.033 ± 0.015 cm/MW. Previous theoretical measurements have yielded TPA coefficients of[1] 0.02 cm/MW and 0.05 cm/MW.[8]

The purpose of this paper is to study the spectral dependence of the two-photon absorption near the band-gap, and hence elucidate the transition mechanism. The luminescence technique is especially well suited for such studies, and we show that the TPA process results from the allowed-forbidden mechanism in the two-band approximation.[9,10] The luminescence technique by itself as it is used here is not capable of yielding quantitative data. Measurements of the TPA attenuation were made using the available laser source with powers up to 15 MW/cm^2 and samples 0.2-cm long confirmed that at 1.6 eV the TPA coefficient was less than 0.015 cm/MW. This is in contrast to a anomalously large value of 1.15 ± 0.05 cm/MW found recently using 1.65-μm radiation.[11] In this case, considerably smaller TPA coefficients were found at shorter wavelengths. This large peak in the TPA was attributed to the presence of an unknown deep impurity level near the middle of the band gap. The spectral dependence of this process differs significantly from the two- or three-band models. Similar effects have also been observed by us, however, they were absent in the work reported here which utilized specially prepared samples having the appropriate purity.

II. THEORY (REFS. 9 AND 10)

The attenuation of a fundamental beam of intensity I_1 at frequency ω_1 is

$$\frac{dI_1}{dz} = -\alpha_1 I_1 - \beta_1 I_1^2, \tag{1}$$

where α_1 is the loss coefficient due to absorption and scattering, and $\beta_1 = (W/VI^2)2\hbar\omega_1$ is the relation between the TPA coefficient and the TPA transition rate W per unit volume V. It is assumed that consecutive absorption processes do not occur, hence only the two-photon process can populate the excited state near $2\omega_1$. The spatial dependence of the beam is important when absolute values of β_1 are to be obtained, but this effect enters as a constant factor in the spectral dependence. The solution of Eq. (1) yields the fraction of the beam attenuation due to two-photon absorption

$$\Delta I_{1\,\mathrm{TPA}} = (\alpha_1/\beta_1)\{[1 + (\beta_1/\alpha_1)I_{10}][1 + g(z)^{-1}]^{-1} - \ln[1 + g(z)]\}, \tag{2}$$

where I_{10} is the intensity at the entrance face of the crystal and

$$g(z) = (\beta_1/\alpha_1)I_{10}(1 - e^{-\alpha_1 z}). \tag{3}$$

For small linear and nonlinear loss values, $\alpha_1 z \ll 1$, $\beta_1 z \ll 1$, Eq. (2) reduces

$$\Delta I_{1\,\mathrm{TPA}} = [\beta_1 I_{10}^2 z/(1 + \beta_1 I_{10} z)](1 - \alpha_1 z). \tag{4}$$

The detected luminescence intensity at ω_L resulting from the two-photon absorption at $2\omega_1$ is

$$I_L = \Delta I_{1\,\mathrm{TPA}} q f(\omega_L/2\omega_1), \tag{5}$$

where q is the quantum efficiency for excitation at $2\omega_1$, which is assumed to be constant over the small range of energy above the gap, and f is the fraction of the collected luminescence which is a function of the geometry.

The TPA coefficient is related to the imaginary part of the nonlinear third-order electric dipole susceptibility tensor[10]

$$\beta_1 = (32\pi^2\omega_1/c^2)\chi''_{ijkl}(-\omega_1, \omega_1, \omega_1, -\omega_1). \quad (6)$$

The III-V compounds have $\bar{4}3m$ symmetry and when all the frequencies in χ'' are the same, there are three independent tensor elements: χ''_{iiii}, χ''_{iijj}, χ''_{ijji}.[12] The tensor character of χ introduces an anisotropy in the two-photon signal. For radiation incident in the [001] direction, and polarized at angle θ with respect to the [100] axis, the angular dependence is given by

$$I_L \alpha \chi''_{xxxx} + \tfrac{1}{2}(2\chi''_{xxyy} + \chi''_{xyyx} - \chi''_{xxxx})\sin^2(2\theta). \quad (7)$$

Expressions for the two-photon excitation rates have been derived in the two-band approximation by Fossum and Chang[13] for InSb and these results are applied here to GaAs. At the temperatures of interest, the heavy- and light-hole valence bands, corresponding to $i = 1$ and 2, respectively, are fully populated and the conduction band is empty. The transition rate above the gap per unit volume is

$$\frac{W_{vi\to c}}{V} = \frac{16\sqrt{2}}{15}\frac{\pi}{\epsilon}\left(\frac{e}{\hbar c}\right)^2 \frac{(C_i Q)^2}{\hbar^4\omega_1^6 m^2} m_{cvi}(2\hbar\omega_1 - E_g)^{3/2} I^2, \quad (8)$$

where the parameters are defined in Refs. 13 and 14 and

$$Q = [\tfrac{3}{2}mE_g(m/m_c - 1)(E_g + \Delta)/(3E_g + 2\Delta)]^{1/2} \quad (9)$$

is the matrix element of the angular momentum operator between the valence and conduction band, and

$$c_1^2 = a_c^2,$$
$$c_2^2 = 3(a_c c_{v2} + c_c a_{v2})^2 + (a_c b_{v2} - b_c a_{v2})^2 \quad (10)$$

describes the wave-function admixture. At the higher energies the split-off valence band with $i = 3$ also contributes to W.[14]

The total transition rates and β_1 were calculated as a function of ω_1. Using the parameters for InSb the transition rates at 2 °K obtained by Fossum and Chang[13] were reproduced. For GaAs, the following parameters were used: $\Delta = 0.34$ eV,[15] $m_c = 0.067m$,[16] $m_{v1} = 0.45m$,[16] $m_{v2} = 0.082m$,[16] $m_{v3} = 0.15m$,[17] and $E_g = 1.424$ eV at 300 °K,[18] $E_g = 1.519$ eV at 4.2 °K.[19] At 1.0642 μm, the calculated TPA coefficient of GaAs at 300 °K, obtained by including the contributions of the light- and heavy-hole bands as well as the split-off valence band is 0.0083 cm/MW. This β_1 is a factor of 4 smaller than the measured value.[7]

There is also a luminescence signal due to the absorbed second-harmonic intensity when the incident radiation is polarized along the [110] axis. The effective two-photon coefficient is given by

$$\beta_{2\omega} = \frac{2\mu_0^{3/2}\epsilon_0^{1/2} d^2\omega_1^2}{n_{2\omega}(n_\omega)^2}\frac{\alpha_2}{(\frac{1}{2}\alpha_2)^2 + (\Delta k)^2}, \quad (11)$$

where we have assumed $\alpha_1 = 0$. For a 1.55 μm (0.8 eV) fundamental we take $d \approx 9\times 10^{-10}$ m/V, $n_{2\omega} = 3.68$, $n_\omega = 3.38$, $\alpha_2 \approx 10^4$ cm^{-1} and find $\beta_{2\omega} \approx 4\times 10^{-5}$ cm/MW. This is small compared with $\beta = 2.1\times 10^{-3}$ cm/MW calculated from the allowed-forbidden mechanism in Eq. (8), and hence the second-harmonic mechanism can safely be neglected in this case.

III. EXPERIMENTAL

The measurements were made using thin films grown on (001) oriented GaAs substrates by liquid-phase epitaxy.[20] Both single-crystal films ~ 100 μm thick as well as heterostructure wave guides having a central 12-μm-thick GaAs region and 3-μm-thick $Al_{0.43}Ga_{0.57}As$ cladding layers were tested. In addition to providing greater confinement of the radiation, the cladding considerably decreases the nonradiative recombination at the GaAs surface. The recombination radiation is close to the surface and is readily transmitted through the $Al_{0.43}Ga_{0.57}As$ cladding so that self-absorption effects are minimized. Hence the luminescence from the guides was considerably more intense than from the single layers.

Small bars 1–2 mm long with $[1\bar{1}0]$ entrance and exit faces were cleaved from the wafer (Fig. 1). The samples were mounted at the tip of a variable temperature cryotip refrigerator. Infrared radiation from a temperature-tuned parametric oscillator is focused by the 3-cm focal-length spherical lens on the front face of the crystal in the direction normal to the film. In the plane of the film the combined cylindrical and spherical lenses focus the radiation in the sample. The parametric oscillator output is linearly polarized and the polarizing prisms serve to attenuate the beam and to define the plane of polarization.

The emitted radiation passing in the [001] direction was collected by a lens filtered to pass only the recombination radiation and detected by a

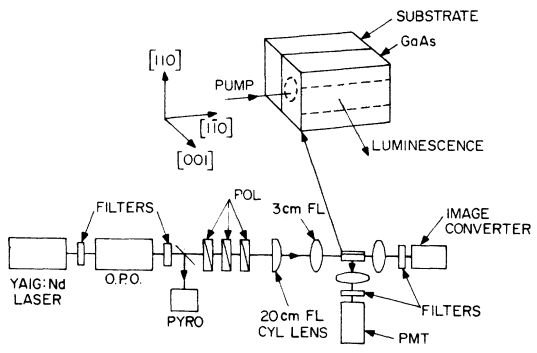

FIG. 1. Experimental arrangement used to observe luminescence due to two-photon absorption.

cooled S-1 response photomultiplier tube. Part of the incident beam was monitored by a rapid-response pyroelectric detector, and electronically squared. We used a ratio of the photomultiplier signal with the square of the monitor signal to reduce the effects of fluctuations of the input beam intensity. The initial focusing of the beam on the guide was obtained using the idler beam near 1 μm and examining the transmitted beam with an infrared image converter tube. The final alignment in the infrared was obtained by optimizing the luminescence signal.

The luminescence signal and its spectral dependence are functions of the temperature at which the layers were grown. While all of the samples were nominally undoped, the intensity from a waveguide sample grown at 850 °C was about a factor of 2 higher than from a similar guide grown at 750 °C. The intensity from these samples increased more rapidly above E_g than the calculated spectrum. Very large luminescence signals were also observed from the substrate material which was compensated with Cd and is nominally p type. The intensity from the single layer samples grown by cooling from 1000 to 950 °C was considerably weaker, and as discussed below had the spectral dependence which agreed with theory. The as-grown surfaces of these samples were relatively rough and were polished smooth using a bromine methanol etch.

The dependence of the intensity on growth temperature is qualitatively explained by the presence of deep levels near the middle of the band resulting from the presence of unknown defects. Deep level transient spectroscopy studies made by Lang[21,22] indicate that there are trap levels 0.4 and 0.71 eV above the valence band. We presume the latter defect leads to the enhancement of the TPA effect. The concentration of the trap levels is a function of the crystal-growth temperature. Thus the concentration of traps in crystals grown at 750 °C is reduced by approximately a factor of 5 relative to crystals grown at 850 °C (Refs. 23 and 24) and for growth at 1000 °C the reduction is approximately a factor of 20.[23] The reduction in the defect concentration at high-growth temperatures has been tentatively attributed to compensation by the unintentional presence of amphoteric Si.[23] The luminescence signals observed in the samples grown at low temperatures are then attributed to the combined effects of intrinsic as well as impurity-induced TPA, while the intrinsic TPA predominates in the samples grown at 1000 °C. These results indicate the necessity of using high-purity samples for studying intrinsic TPA. The use of impure samples may in part explain the wide range of previously measured TPA values.

IV. RESULTS

The calculated transition rates at 300 and 4 °K for $I = 1$ MW/cm^2, as a function of the two-photon energy, are given by the curves in Fig. 2. The points are obtained from the experimental luminescence traces for [001] incident polarization, and for each curve the points were multiplied by constant numerical factors to obtain the coincidence with the theoretical curves. The agreement is reasonable over most of the spectral range indicating the allowed-forbidden (two-band) model gives a good description of two-photon absorption well above the band gap. Above 1.65 eV the measured luminescence data is up to ~10% below the calculated transition rate. Since the effect appears at the same energy for both sample temperatures, it seems reasonable to tentatively attribute this deviation to a change in the output characteristics of the parametric oscillator spectrum as its degeneracy point is approached rather than to a change in the transition rate. The deviation of the 300 °K data near the band edge is attributed to the broadening of the band gap, and the bump near the gap in the low-temperature data is due to exciton effects.

The structure near the band gap for both polarizations is shown in more detail in the semilog traces in Fig. 3. The points give the calculated spectrum from Eq. (8) and were fitted to the experimental data using $E_g = 1.519$ eV.[19] The agreement with the two-band model is quite reasonable, except for the initial region up to ~10 meV above

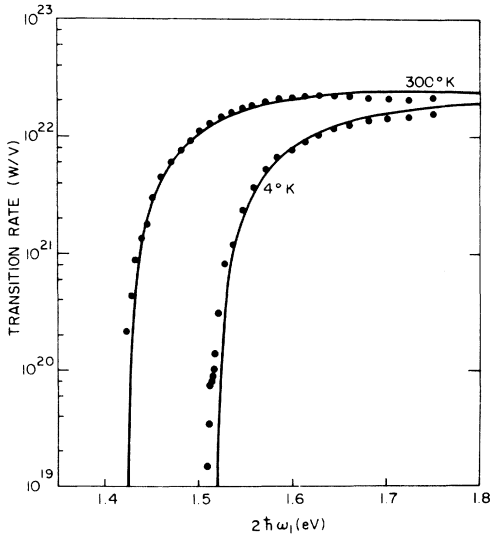

FIG. 2. Curves are the two-photon transition rates calculated from Eq. (8) for $I_1 = 1$ MW/cm^2 as a function of twice the pump energy. The points are obtained from the experimental luminescence traces.

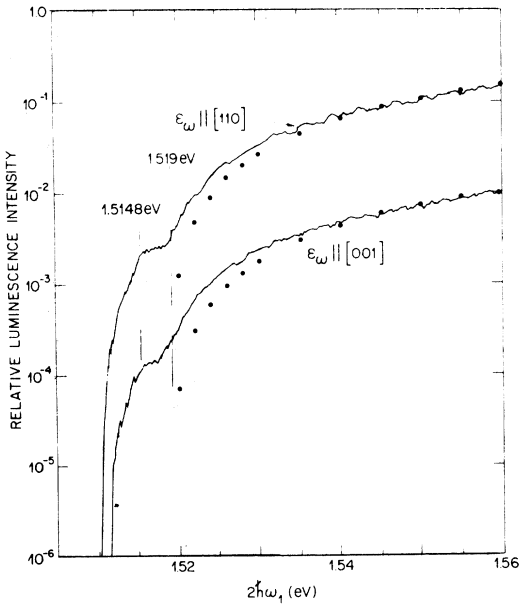

FIG. 3. Luminescence traces due to two-photon absorption near the band gap for pump polarization along the [110] and [001] axes. The curves have been arbitrarily displaced to show detail. The points are the calculated two-photon transition rates for the two-band model and are placed to optimize the fits to the experimental curve.

the band gap where the measured signals are larger than the calculated values. The difference is attributed to the allowed-allowed mechanism corresponding to the three-band model which has an approximately $(2\hbar\omega - E_g)^{1/2}$ spectral dependence,[9] and to exciton contributions in the continuum.[9] To illustrate this more clearly the 4 °K data of Fig. 2 are plotted in Fig. 4 on a log-log scale. The two- and three-band contributions are equal ~2 meV above the band gap. For the two-band contribution accurate proportionality is found for the limited range only up to 30 meV above the band gap. Between 30 and 100 meV both the $(\hbar\omega_1)^{-6}$ dependence and the change in the matrix elements due to the variation in the wave-function admixture contribute about equally to the deviation from the $\frac{3}{2}$ power dependence. Above 100 meV the effect due to the $(\hbar\omega_1)^{-6}$ dependence dominates.

The excitons appear in both polarizations in Fig. 3. The exciton structure is found to be 4.2 meV from the band gap which agrees with the 4.2-meV binding energy of the $n = 1$ exciton observed in absorption.[25-27] We note that in the two-band model the "allowed" two-photon transition occurs to the final p exciton states and bands and are forbidden to the $n = 1$ excitons because these have only s-like envelopes.[28-30] In the three-band model the allowed two-photon transitions will occur to the s state exciton envelopes and bands including the $n = 1$ exciton.[29-31] The relatively large observed transition strength of the $n = 1$ exciton is thus identified with the three-band model.

The angular dependence of the two-photon effect was obtained with the laser beam directed approximately along the [001] normal of the epilayer. A small offset in the horizontal plane was necessary to efficiently collect the luminescence. The incident beam was polarized in the vertical plane. When the polarization was along the [110] axis a second-harmonic polarization is produced along the [001] axis, which does not radiate and hence should not contribute to the signal.

The luminescence at $2\hbar\omega_1 = 1.6$ eV was recorded as the plate was rotated about the [001] axis by a motor drive. The points in Fig. 5 show the intensity, on an arbitrary scale, obtained at 10° intervals from the recorded trace. The curve is a plot of Eq. (7) with parameters obtained from a least-squares fit to the data points. This fit yields a value for the anisotropy

$$(2\chi''_{xxyy} + \chi''_{xyyx})/\chi''_{xxxx} = 1.45 \pm 0.06. \qquad (12)$$

For isotropic media this ratio is unity by symmetry. A similar anisotropy has been observed at 1.064 μm.[32] The real parts of the third-order purely electronic susceptibility have previously

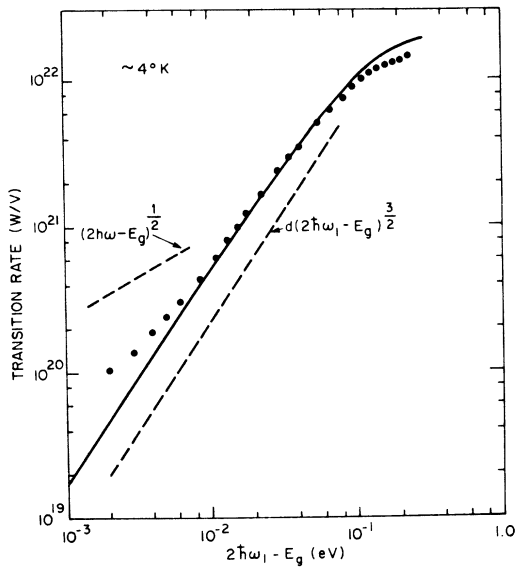

FIG. 4. Plot of the calculated two-photon transitions rate (curve) and the low-temperature experimental data from Fig. 2 (points) showing the $(2\hbar\omega_1 - E_g)^{3/2}$ and $(2\hbar\omega - E_g)^{1/2}$ power dependences. The deviation well above the band gap results from the $(\hbar\omega_1)^{-6}$ dependence and the effect of the change in wave-function admixture on the matrix element.

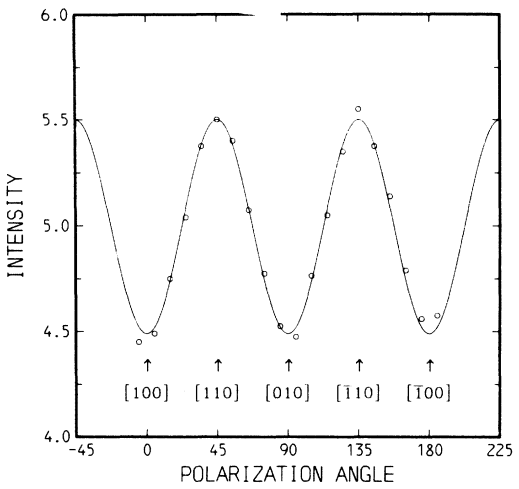

FIG. 5. Dependence of the luminescence intensity on the polarization of the incident beam as the sample is rotated about [001]. The curve is the calculated fit to the experimental points.

been measured in a three-wave mixing experiment where $\omega_3 = 2\omega_1 - \omega_2$ using two tunable CO_2 lasers.[33] The ratio was found to be

$$3\chi'_{xyxy}/\chi'_{xxxx} = 1.59 \pm 10\%. \quad (13)$$

A first-principle calculation of the third-order nonlinear susceptibility has yielded a value of 1.5 for this ratio.[34] Thus the ratios of the tensor components for the real and imaginary parts are essentially equal, and hence χ_{xxyy} is a constant fraction of χ_{xxxx}.

V. SUMMARY

We have used the fluorescence technique to show that in pure GaAs the two-band process dominates the two-photon process for energies well above the band gap and the three-band process dominates just above the band gaps. The weak transition to the $n = 1$ exciton is attributed to the three-band process. The angular dependence of the TPA yields a value for the ratio of the components of the imaginary part of the $\chi^{(3)}$ which are the same as the measured and calculated ratios of the real part of $\chi^{(3)}$.

ACKNOWLEDGMENTS

The author wishes to thank R. A. Logan and H. G. White for growing the epitaxial layers and R. M. Mikulyak for experimental assistance.

[1]N. G. Basov, A. Z. Grasiuk, V. F. Efimov, I. G. Zubarev, V. A. Katulin, and J. M. Popov, J. Phys. Soc. Jpn. Suppl. 21, 227 (1966).
[2]V. V. Arsen'ev, V. S. Dneprovskii, D. N. Klysko, and A. N. Penin, Zh. Eksp. Teor. Fiz. 56, 760 (1969). [Sov. Phys.-JETP 29, 413 (1969)].
[3]J. M. Ralston and R. K. Chang, Appl. Phys. Lett. 15, 164 (1969); Opto-Electron 1, 182 (1969).
[4]C. C. Lee and H. Y. Fan, Appl. Phys. Lett. 20, 18 (1972).
[5]S. Jayaraman and C. H. Lee, Appl. Phys. Lett. 20, 392 (1972).
[6]J. M. Bechtel and W. L. Smith, Phys. Rev. B 13, 3515 (1976).
[7]D. A. Kleinman, R. C. Miller and W. A. Nordland, Appl. Phys. Lett. 23, 243 (1973).
[8]L. V. Keldysh, Zh. Eksp. Teor. Fiz. 47, 1945 (1964) Sov. Phys.-JETP 20, 1307 (1965).
[9]V. I. Bredikin, M. D. Galanin and V. N. Genkin, Usp. Fiz. Nauk 110, 3 (1973) [Sov. Phys.-Usp. 16, 299 (1973)].
[10]H. Mahr, in *Quantum Electronics*, edited by H. Rabin and C. L. Tang (Academic, New York, 1975), Vol. IA, p. 285.
[11]A. Z. Grasyuk, I. G. Zubarev, A. B. Mironov, and I. A. Poluektov, Fiz. Tekh. Poluprovodn. 10, 262 (1976) [Sov. Phys.-Semicond. 10, 159 (1976)].
[12]C. Flytzanis, in Ref. 10, p. 1.
[13]H. J. Fossum and D. B. Chang, Phys. Rev. B 8, 2842 (1973).
[14]E. O. Kane, J. Phys. Chem. Solids 1, 249 (1957).
[15]O. Berolo and J. C. Woolley, in *Proceedings of the Eleventh International Conference on the Physics of Semiconductors* (Polish Scientific, Warsaw, 1972), Vol. 2, p. 1420.
[16]Q. H. F. Vrehen, J. Phys. Chem. Solids 29, 129 (1968).
[17]P. Lawaetz, Phys. Rev. B 4, 3460 (1971).
[18]D. D. Sell, H. C. Casey, Jr., and K. W. Wecht, J. Appl. Phys. 45, 2650 (1974).
[19]C. D. Thurmond, J. Electrochem. Soc. 122, 1133 (1975).
[20]R. A. Logan and F. K. Reinhart, IEEE J. Quant. Electron. 11, 461 (1975).
[21]D. V. Lang and R. A. Logan, J. Appl. Phys. 47, 1533 (1976).
[22]D. V. Lang and R. A. Logan, J. Electron. Mater. 4, 1053 (1976).
[23]D. V. Lang (private communication).
[24]T. Uji and K. Nishida, Jpn. J. Appl. Phys. 15, 2247 (1976).
[25]D. D. Sell, Phys. Rev. B 6, 3750 (1972).
[26]D. D. Sell, S. E. Stokowski, R. Dingle, and J. V. DiLorenzo, Phys. Rev. B 7, 4568 (1973).
[27]S. B. Nam, D. C. Reynolds, C. W. Litton, R. J. Almassy, T. C. Collins, and C. M. Wolfe, Phys. Rev. B 13, 761 (1976).
[28]G. D. Mahan, Phys. Rev. Lett. 20, 332 (1968); Phys. Rev. 170, 825 (1968).
[29]V. I. Bredikhin and V. N. Genkin, Fiz. Tverd. Tela 11, 2317 (1969) [Sov. Phys.-Solid State 11, 1871 (1970)].

[30]E. Doni and G. P. Parravicini, Solid State Commun. 14, 873 (1974).
[31]M. Inoue and Y. Toyazawa, J. Phys. Soc. Jpn. 20, 363 (1965).
[32]S. J. Bepko, Phys. Rev. B 12, 669 (1975).
[33]E. Yablonovitch, C. Flytzanis, and N. Bloembergen, Phys. Rev. Lett. 29, 865 (1972).
[34]C. Flytzanis, Phys. Lett. A 31, 273 (1970).